Received: 25 June 2018 | Revised: 9 October 2018 | Accepted: 9 October 2018

DOI: 10.1111/adb.12692

ORIGINAL ARTICLE

WILEY Addiction Biology SSA

Shifts in the functional topography of frontal cortex-striatum connectivity in alcohol use disorder

Martin Fungisai Gerchen[1,3] | Alena Rentsch[1] | Martina Kirsch[2] | Falk Kiefer[2] | Peter Kirsch[1,3]

[1] Department of Clinical Psychology, Central Institute of Mental Health, University of Heidelberg/Medical Faculty Mannheim, Mannheim, Germany

[2] Department of Addiction Behavior and Addiction Medicine, Central Institute of Mental Health, University of Heidelberg/Medical Faculty Mannheim, Mannheim, Germany

[3] Bernstein Center for Computational Neuroscience Heidelberg/Mannheim, Mannheim, Germany

Correspondence
Martin Fungisai Gerchen, Department of Clinical Psychology, Bernstein Center for Computational Neuroscience Heidelberg/Mannheim, Central Institute of Mental Health (ZI), University of Heidelberg/Medical Faculty Mannheim, J5, Mannheim 68159, Germany.
Email: martin.gerchen@zi-mannheim.de

Funding information
Bundesministerium für Bildung und Forschung, Grant/Award Numbers: 01GQ1003B and 01ZX1311A; Horizon 2020 Framework Programme, Grant/Award Number: No 668863 (SyBil-AA); Deutsche Forschungsgemeinschaft, Grant/Award Number: SFB 636/D6

Abstract

Frontostriatal circuits are centrally involved in the selection of behavioral programs and play a prominent role in alcohol use disorder (AUD) as well as other mental disorders. However, how frontal regions change their striatal connectivity to implement adaptive cognitive control is still not fully understood. Here, we developed an approach for functional magnetic resonance imaging (fMRI) connectivity analysis in which we change the focus from connectivity to individual voxels towards spatial information about the location of strongest functional connectivity. In resting state data of n = 66 participants with AUD and n = 40 healthy controls (HC) we used the approach to estimate frontostriatal connectivity gradients consistent with nonhuman primate tract-tracing studies, characterized for each frontal voxel the striatal peak connectivity location on this gradient (PeaCoG), and tested for group differences and associations with clinical variables. We identified a cluster in the right orbitofrontal cortex (rOFC) with a peak connectivity shift towards ventral striatal regions in AUD. Reduced variability of rOFC striatal peak connectivity in the AUD group suggests a "clamping" to the ventral striatum as the underlying effect. Within the AUD group striatal peak connectivity in the superior frontal gyrus was associated with self-efficacy to abstain from alcohol, in the medial frontal and dorsolateral prefrontal cortex with alcohol dependency, and in the right inferior frontal gyrus with the urge to consume alcohol. Our results demonstrate that the functional topography of frontostriatal circuits exhibits interindividual variability, which provides insight into frontostriatal network adaptations in AUD and potentially other mental disorders.

KEYWORDS

alcohol addiction, cognitive control, functional magnetic resonance imaging, resting state, top down, ventral striatum

1 | INTRODUCTION

One of the central aspects of healthy human behavior is the appropriate selection of behavioral programs, be they motor, cognitive, affective, or reward related. Especially disorders of addiction like alcohol use disorder (AUD), but to a certain degree, almost all mental disorders are characterized by an inflexible selection and a loss of control over (overt or covert) behavior.

Central brain circuits involved in the selection of behavioral programs are frontal cortex-basal ganglia-thalamus-frontal cortex loops.[1-3] Neurobiological models of AUD postulate that a dysfunction between increased reward system and decreased executive control

activation results in addiction-related behaviors such as compulsive and impulsive use of alcohol.[4,5] Cumulating research in AUD suggests that dysfunctional inhibitory control results from aberrant top-down regulation of the prefrontal cortex over the striatum.[5-9]

Resting state functional magnetic resonance imaging (fMRI) studies where participants passively lie in the scanner without a task have further identified changes in frontostriatal connectivity in AUD. For example, a study by Camchong et al[10] compared AUD patients who relapsed with those who abstained from alcohol and found decreased functional connectivity between the ventral striatum and the dorsolateral prefrontal cortex (DLPFC), which was associated with poorer inhibitory control. Müller-Oehring et al[11] found expanded nucleus accumbens (NAcc) connectivity with bilateral medial and inferior prefrontal gyri (PFG) in AUD patients with more expanded NAcc-medial PFG connectivity, correlating with higher-trait anxiety scores. Using probabilistic independent component analysis, Zhu et al[12] found increased within network functional connectivity in AUD patients in orbitofrontal and amygdala-striatum networks that included parts of the striatum.

In contrast, long-term abstinent AUD patients, who successfully abstained from alcohol showed higher connectivity of the ventral striatum with the inhibitory control network including the DLPFC and reduced connectivity with the appetitive drive reward network in comparison with nonsubstance abusing controls, which was associated with cognitive flexibility in a set shifting task.[13]

However, how frontostriatal circuits are functionally implementing flexible cognitive control is still not fully understood.

Frontostriatal organization has been described on the broad scale as a tripartite separation into dorsal motor, medial cognitive, and ventral affective/reward-related circuits.[1,3] While ventral circuits have been associated with motivational salience and goal-directed behavior, more dorsal circuits have been associated with habitual behavior, and a shift from more ventral to more dorsal striatal processing likely plays a central role in the development of addictions.[14,15] Together, frontostriatal circuits are forming a functional hierarchy that integrates reward-related information with cognitive planning capabilities to control the execution of motor programs.[2]

On a finer level, frontostriatal topography follows a gradient with medial-lateral, ventral-dorsal, and rostral-caudal direction components,[1-3] which can also be identified in diffusion-weighted tractography and functional connectivity fMRI studies.[16-21]

Here, we develop an analysis approach aiming at extracting information from fMRI data reflecting the fine topography of frontostriatal connectivity as described in Haber[1] to make this information accessible for testing and interpretation. Therefore, we changed the focus of analysis from connectivity to individual voxels or regions (as in most conventional fMRI analyses), to the spatial location of strongest (peak) functional connectivity. The first step of our method consists of identifying the location with highest functional connectivity in the striatum for every frontal voxel. This spatial information is then used to empirically estimate a frontostriatal connectivity gradient. The position of striatal peak connectivity on this gradient provides a single value for each frontal voxel, representing where it has the highest functional connectivity in the striatum.

Importantly, the concept of separate frontostriatal circuits does not imply that cortical regions are strictly connected to a single striatal locus.[2,3] Instead, cortical connections to the striatum have distributed patterns in which connections of a given cortical region to the striatum are spread out and overlap with projections from other cortical regions.[16,17,22-27]

On the basis of a comprehensive review of the literature, Shipp[3] argues that corticostriatal projections follow an organizational principle of both segregation and integration that is probably best described as "disclosed loops." In this model, cortical regions are the origin of cortex-basal ganglia-thalamus-cortex loops that terminate at the cortical origin as well as of moderating connections projecting to striatal loci, which are part of loops terminating at other cortical locations. Corticostriatal projections leading to closed loops are called "operative," while projections to other striatal areas are called "contextual." It is through these contextual projections that cortical regions can exert influence on other operative circuits related to diverse cognitive functions. Hence, we hypothesize that functional connectivity of frontal regions to the striatum can vary depending on whether they are in an "operative" or "contextual" mode.

The peak connectivity estimates provided by our approach can be used to conduct statistical tests over the striatal projections of frontal voxels, which enables us to identify such changes and map frontal cortex regions where frontostriatal peak connectivity locations are systematically associated to interindividual differences. As a first application, we apply the method to gain insight into functional changes in the frontostriatal topography in alcohol addiction.

2 | MATERIALS AND METHODS

2.1 | Study and participants

Resting state data of 123 subjects were acquired. We excluded two subjects for anatomical anomalies, five for missing physiological data, four for excessive head motion (>3 mm movement or >33% small movement affected volumes), and six subjects for restricted coverage of the brain in normalized functional data. The final analyzed sample included N = 106 participants, n_{AUD} = 66 (16 female) with AUD and n_{HC} = 40 (17 female) healthy controls (HC). Mean age did not differ between the groups (AUD: 46.8 ± 9.16 years (mean ± standard deviation [SD], range 25-65 y; HC: 47.28 ± 9.21 y, range 22-64 y; two sample t test t = 0.2566, P = 0.798), but a trend towards a higher ratio of female participants in the HC group was present (Fisher's exact test P = 0.052). Therefore, we conducted group comparisons with the whole sample first but repeated the analyses after exclusion of female participants.

Patients were recruited from the Central Institute of Mental Health (CIHM) inpatient clinic. Trained psychologists diagnosed alcohol addiction based on the International Classification of Disease (ICD-10) and the Diagnostic and Statistical Manual of Mental Disorders (DSM-IV). Other mental disorders were assessed by the Structured Clinical Interview for DSM-IV (SCID-I[28]). Verified by urine drug testing, patients did not consume any other drugs, benzodiazepine, or chlormethiazole. Prior to scanning participants were abstinent for at

least 5 days and, if necessary, complete a medically supervised detoxification program. Participants were scanned only if they were free of any detoxification medicine for 3 days. On average, patients abstained from alcohol prior to scanning for 10.12 ± 4.69 days (mean ± SD, range: 5-31 d). Before fMRI, all participants completed questionnaires including the Obsessive Compulsive Drinking Scale (OCDS[29]), Alcohol Abstinence Self-Efficacy Scale (AASE[30]), Alcohol Dependence Scale (ADS[31]), and the Alcohol Urge Questionnaire (AUQ[32]).

The study was approved by the ethics committee of the Medical Faculty Mannheim, University of Heidelberg, Germany (2011-303 N-MA), and procedures complied with the WHO's Declaration of Helsinki. Before participation, all participants were educated about the study and provided written informed consent. Participants received 50 € for scanning.

The analyzed resting state data were acquired in the baseline MRI session of a larger study.[33,34] The reported analyses are exploratory and were not originally planned for the study. The difference in group size is due to the existence of two clinical groups and one control group in the original experiment.

2.2 | Functional magnetic resonance imaging

Anatomical and resting state functional images were acquired as the first two scans of the baseline session with a 3 T Siemens Trio TiM scanner (Siemens Healthineers, Erlangen, Germany) at the CIMH. MPRAGE images were acquired with a repetition time (TR) of 2.3 seconds, an echo time (TE) of 3.03 ms, a flip angle of 9°, and a resolution of 1 × 1 × 1 mm. In the 5:30 minutes resting state session, we acquired 220 functional echo-planar imaging (EPI) images with a TR of 1.5 seconds, a TE of 28 ms, and a flip angle of 80° in 24 slices of 4 mm thickness with 1 mm gap and in-plane resolution of 3 × 3 mm. During functional imaging respiration and heart rate were monitored with scanner built-in equipment.

2.3 | Statistical analyses

Statistical analyses were conducted with SPM12 (v6685; Wellcome Department of Cognitive Neurology, London, United Kingdom) and in-house scripts running in MATLAB (R2011b; MathWorks Inc., Sherborn, Massachusetts, United States).

2.4 | fMRI preprocessing

Preprocessing included segmentation of the MPRAGE and normalization onto SPM12's TPM templates in MNI space. Correction for physiological artifacts was conducted with AZTEC based on heart rate and respiration data acquired during scanning. AZTEC uses RETROICOR and linear modelling of respiration volume, heart rate, and heart rate variability.[35] Functional data were slice-time corrected, realigned to the mean image, coregistered to the anatomical image, normalized by applying forward deformation fields estimated during normalization of the MPRAGE, resampled to 2 × 2 × 2 mm, and smoothed with a FWHM = 6 × 6 × 6 mm Gaussian kernel.

2.5 | Resting state analyses: first level

Analyses were implemented in SPM12 with two consecutive first level analyses. The "first" first level analysis was conducted to extract white matter (WM), cerebrospinal fluid (CSF), and global signals and identify volumes affected by small scan-to-scan movements (movement threshold = 1 mm; z = 5) with the ART-toolbox (http://www.nitrc.org/projects/artifact_detect). In this step, we included the six standard movement parameters and performed analyses without prewhitening (autocorrelation correction), which is applied to the covariate time courses in the next step. In the "second" first level we conducted analyses with prewhitening (AR [1]) and included as covariates the six movement parameters, WM, CSF, global signal, and dummy regressors for small motion-affected volumes. For WM, CSF, and global regressors, we used the eigenvariate extracted from WM, CSF, and global masks, respectively. The dummy regressors implement a spike regression procedure that controls for the effect of small movements. A high-pass filter with a cutoff of 128 seconds was used in first levels. The residual time series from the second first level corrected for the nuisance effects were used for connectivity analyses.

The number of motion-effected volumes did not differ significantly between the groups, although the value is nominally slightly higher in the clinical group (AUD: 2.62 ± 4.9% HC: 1.73 ± 4.8%; two sample t test: t = 0.91, P = 0.36).

2.6 | Masks

We constructed masks of the striata and the frontal cortices (Figure S1) based on the Neuromorphometrics (NMM) atlas (http://Neuromorphometrics.com/). We used this atlas because it is distributed with SPM12 and is registered to the exact space of the SPM12 TPM template. The striatum mask included the NMM masks for caudate, putamen, and accumbens area. For a list of all regions in the frontal masks, see Supplementary Table 1. Of note, we included the anterior insula and the anterior cingulate cortex in the frontal cortex mask.

To account for potential biases in normalization because of inter-individual differences in the size of brain structures, we included individual mask sizes as covariates in group analyses. Frontal and striatal maps were projected into individual subject's anatomical space by using inverse projections obtained during normalization of the MPRAGE. The voxels in the individual masks were counted to estimate mask sizes.

2.7 | Peak functional connectivity location

In each subject, functional connectivity between voxels in the frontal cortex and the striatum was estimated by Pearson correlation. For each voxel in the frontal cortex, the voxel in the striatum with highest functional connectivity was identified, and 3D MNI coordinates of this striatal voxel representing the frontal voxels' striatal peak connectivity location were saved. All analyses were conducted separately in the left

and right hemisphere to avoid mixing up or averaging striatal locations across hemispheres.

2.8 | Principle component analysis

We applied a principle component analysis (PCA) approach to reduce the three spatial MNI dimensions to a single representative axis. In a set of data points, PCA identifies linearly independent dimensions, which are each explaining the largest possible amount of variance. These dimensions, or principle components (PC), are ordered with respect to variance they explain, and selecting the 1st PC provides the dimension explaining the largest variance. For our analyses, we first averaged the peak connectivity locations of each frontal voxel over subjects. Then, we conducted a PCA over all frontal voxels and selected the 1st PC. This component represents the axis along which averaged striatal peak connectivity location varied most across frontal cortex, or, in other words, a frontostriatal connectivity gradient. MNI coordinates of striatal voxels can then be projected onto this gradient, resulting in a single value. Maps of these values for striatal voxels and the averaged striatal peak connectivity location of each frontal voxel are presented in Figure 1. In our analyses, positive values represent lateral-dorsal-caudal and negative values medial-ventral-rostral striatal locations, but direction of axes is arbitrary in PCA. For group level analyses, we projected for each participant all frontal voxels' striatal peak connectivity locations on the gradient (PeaCoG values) and saved them as maps of frontal voxels containing the PeaCoG values (Figure S2).

2.9 | Group level analyses

In all second level analyses age, sex, and the estimated individual size of the striatum and the frontal cortex were included as covariates. Analyses were conducted with SPM12 general linear models (GLM) first. Because PeaCoG values might violate the assumptions of the parametric tests applied by SPM we repeated the analyses with nonparametric permutation tests with FSL's "randomise" function.[36]

2.10 | Group comparison

Frontal PeaCoG maps were first compared between groups with two-sample *t* tests in SPM12. As detection threshold we used a cluster-level threshold of $P = 0.025$ ($P = 0.05$ adjusted for two hemispheres) with a cluster-defining threshold (CDT) of $P = 0.001$ uncorrected. Additional analyses were conducted with a voxel wise FWE-corrected threshold of $P = 0.05$ within the left and right frontal cortices. In the nonparametric permutation tests, we used threshold-free cluster enhancement analysis (TFCE)[36,37] with a corrected threshold of $P = 0.05$ and a voxel wise peak-level analysis with a corrected threshold of $P = 0.05$ within the left and right frontal cortices. After detection of a significant cluster, we extracted covariate-corrected first eigenvariates from the cluster and estimated the cluster-level effect size (Cohen's *d*). Post-hoc inspection of the extracted values hinted at a systematic difference in the variability of PeaCoG values between the groups, which was verified by a post-hoc Brown-Forsythe test for variance homogeneity.[38] The Brown-Forsythe test is a modification of Levene's test and uses an *F* test over absolute deviations from cell medians instead of means, which makes it more robust for deviations from normality and different group sizes (Brown and Forsythe[39]).

Although we used sex as a covariate in the full analysis, we repeated the group comparison with males only ($N = 73$, $n_{AUD} = 50$, $n_{HC} = 23$) as a more rigorous control for confounding effects from the higher ratio of females in the control group.

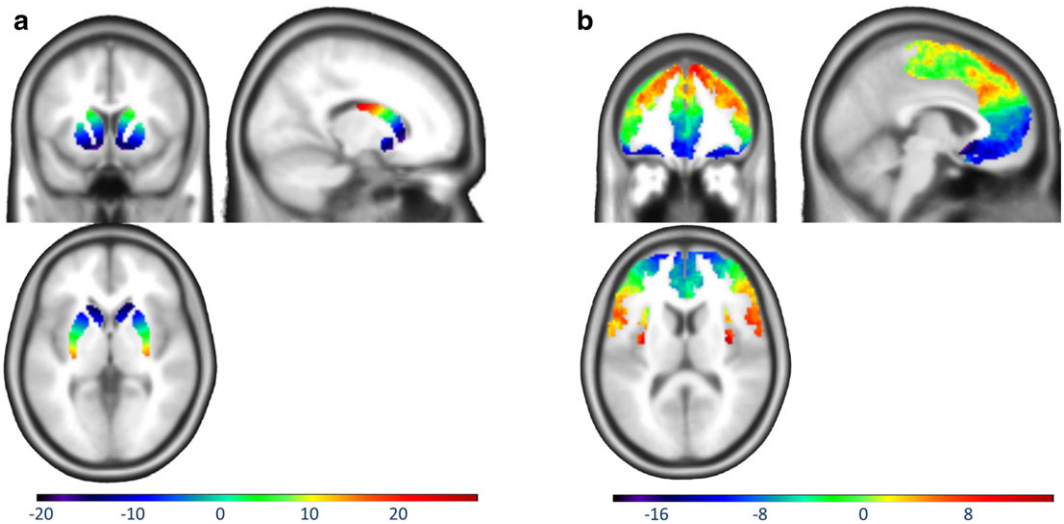

FIGURE 1 Frontostriatal connectivity gradients. Maps of striatal MNI coordinates projected on the estimated frontostriatal connectivity gradients (1st principle component) for (a) the location of voxels in the striatum and (b) the mean locations of peak connectivity in the striatum of frontal voxels. The units of the scales are spatial units representing a linear combination of the axes of the MNI coordinate system (in mm). The color of frontal voxels represents the location in the striatum they were maximally connected to. The hemispheres were analyzed independently. Please note that likely due to the use of averaged values, the dynamic range of the scale in b is more restricted than in a but was used for illustrative purposes

2.11 | Association with clinical variables and test scores

To gain further insight into the clinical relevance of changes in the location of striatal peak connectivity of frontal regions, we associated the PeaCoG values with clinical questionnaire scores in the AUD group by second level SPM regression analyses. Here, we applied the same statistical thresholds as in the group comparison and again repeated the analyses with nonparametric permutation tests. We conducted analyses with eight different clinical scores: 3 scores of the OCDS, 3 scores of the AASE, the ADS sum score, and the AUQ sum score. Please note that we report results with uncorrected nominal significances. The nominal statistical significance threshold Bonferroni corrected for multiple comparisons for cluster-level inference is $P = 0.025/8 = 0.003$. Because participants with missing scores were excluded from the respective tests, these analyses composed between $n = 61$ and $n = 64$ participants with AUD.

Additionally, we tested for an association of clinical variables with the PeaCoG values extracted from the cluster identified in the group comparison.

3 | RESULTS

The first principle component of the PCA over averaged frontostriatal peak connectivity locations in the striatum explains 65.9%/64.2% (left/right hemisphere) of the variance and shows a medial-ventral-rostral (lower values) to lateral-dorsal-caudal (higher values) gradient direction in both striata (Figure 1A). By projecting 3D MNI coordinates of the location of peak connectivity in the striatum onto the gradient, we obtained a single PeaCoG value for each frontal voxel, which we mapped on the frontal cortex. Within subjects, these maps exhibited a "patchy" pattern of regions with relatively similar connectivity (Figure S2). Over participants, PeaCoG values of frontal voxels in the striatum exhibited a substantial amount of variation, with a higher standard deviation in dorsal parts of the frontal cortex, distinguishing them from more ventral regions (Figure S3). Mean PeaCoG shows a ventral-to-dorsal gradient in the ventral part of the frontal cortex and a tendency towards more central striatal peak connectivity in dorsal regions of the frontal cortex (Figure 1B).

3.1 | Group comparison

Comparing frontal PeaCoG maps between groups allows us to ask the question whether frontal regions show systematic connectivity differences along the striatal gradient. We identified a significant cluster in the right orbitofrontal cortex (rOFC) with significantly lower values in the AUD group (cluster-level $P = 0.008$, $k = 19$; peak-level $P = 0.044$ FWE corr.; cluster effect size: Cohen's $d = 1.05$; Table 1 & Figure 2 A). Nonparametric permutation tests provided similar results at the same location (TFCE $P < 0.05$ corr., four voxels; peak-level: $P = 0.048$ corr. [MNI: 22, 42, −16 mm]).

Importantly, a visual inspection of the PeaCoG values of the identified cluster suggests that healthy control participants showed higher variability in rOFC striatal peak connectivity (Figure 2B). A post-hoc Brown-Forsythe test supports this impression ($F = 23.34$, $P < 0.001$).

TABLE 1 SPM results. Results of the group comparison and the association with clinical variables. Cluster defining threshold (CDT) for cluster-level inference: $P = 0.001$ unc. The table shows three local maxima more than 8.0 mm apart

	Cluster Level		Peak Level		
	$p_{FWE\text{-}corr}$	k_E	$p_{FWE\text{-}corr}$	t	MNI (mm; x, y, z)
Group comparison	0.008	19	0.044	4.82	22, 42, −16
AASE Z (negative)	<0.001	30	0.014	5.37	22, 6, 60
				3.28	18, 14, 62
ADS sum (positive)	0.013	17		4.71	6, 30, 34
	0.017	16		4.55	20, 46, 38
	0.002	25		4.45	14, 54, 34
AUQ sum (negative)	<0.001	65	0.033	5.11	48, 22, −8
				4.77	52, 18, −2
				4.49	42, 18, 0

Because the ratio of female participants showed a trend to be higher in the HC group in the included sample, we repeated the analyses after excluding females. While we were not able to cross the detection threshold in the SPM analysis anymore, the effect size in the rOFC cluster diminished only slightly (Cohen's $d = 0.95$ in comparison to $d = 1.05$), and a post-hoc ROI analysis restricted to the cluster remained significant (peak-level $t = 3.63$, $P = 0.003$ FWE-ROI corr., MNI: 26, 44, −12). Importantly, our observation of reduced PeaCoG variability in the rOFC cluster was still highly significant (Brown-Forsythe test $F = 13.19$, $P < 0.001$; Figure S4).

3.2 | Association with clinical questionnaires in AUD

We observed significant effects for three clinical variables in the right hemisphere (Table 1; Figure 3). Again, SPM analyses and nonparametric permutation tests provided similar results. The AASE self-efficacy to abstain scale (AASE-S) was associated with more ventral PeaCoG in a cluster in the superior frontal gyrus (cluster-level $P < 0.001$ corr., $k = 30$; peak-level $P = 0.014$ FWE corr.; permutation tests: TFCE $P < 0.05$ corr., nine voxels; peak-level $P = 0.0173$ corr., MNI: 22, 6, 60). The ADS sum score was associated with more dorsal PeaCoG in three clusters in the medial frontal and dorsolateral prefrontal cortex (cluster-level $P < 0.013$ corr., k = 17; $P < 0.017$ corr, $k = 16$; $P < 0.002$ corr., $k = 25$; peak-level: not significant [*ns*]). In the permutation tests, TFCE analysis identified the same clusters together with some additional effects in the medial frontal cortex (TFCE $P < 0.05$ corr, 215 voxels), and peak-level analyses did also not detect significant effects. The AUQ sum score was associated with more ventral PeaCoG in a cluster in the right inferior frontal gyrus (cluster-level $P < 0.001$ corr., $k = 65$; peak-level $P = 0.033$ FWE corr.; permutation tests: TFCE $P < 0.05$ corr., 99 voxels; peak-level $P = 0.0188$ corr., MNI: 48, 22, −8).

We did not find any association with clinical variables in the rOFC. Also, the first eigenvariates of the PeaCoG values in the rOFC cluster

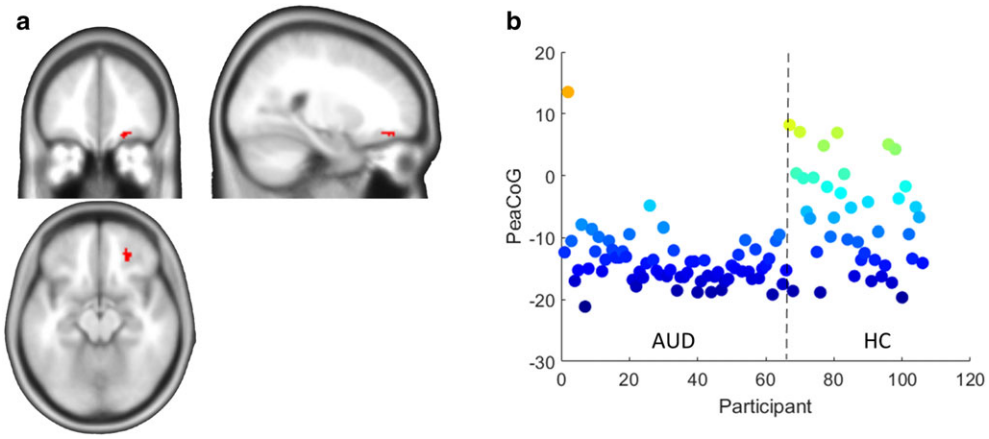

FIGURE 2 Group comparison. (a) Cluster in the right orbitofrontal cortex where striatal peak connectivity location was lower in the AUD group in comparison with the HC group (cluster-level $P < 0.025$ corr.). (b) Individual striatal peak connectivity location on the gradient (PeaCoG) values of the cluster for each participant. The dashed line separates the AUD and HC group. The groups are clearly differing in PeaCoG variability with a more restricted pattern in the AUD group. The color scale corresponds to the striatal gradient in Figure 1A

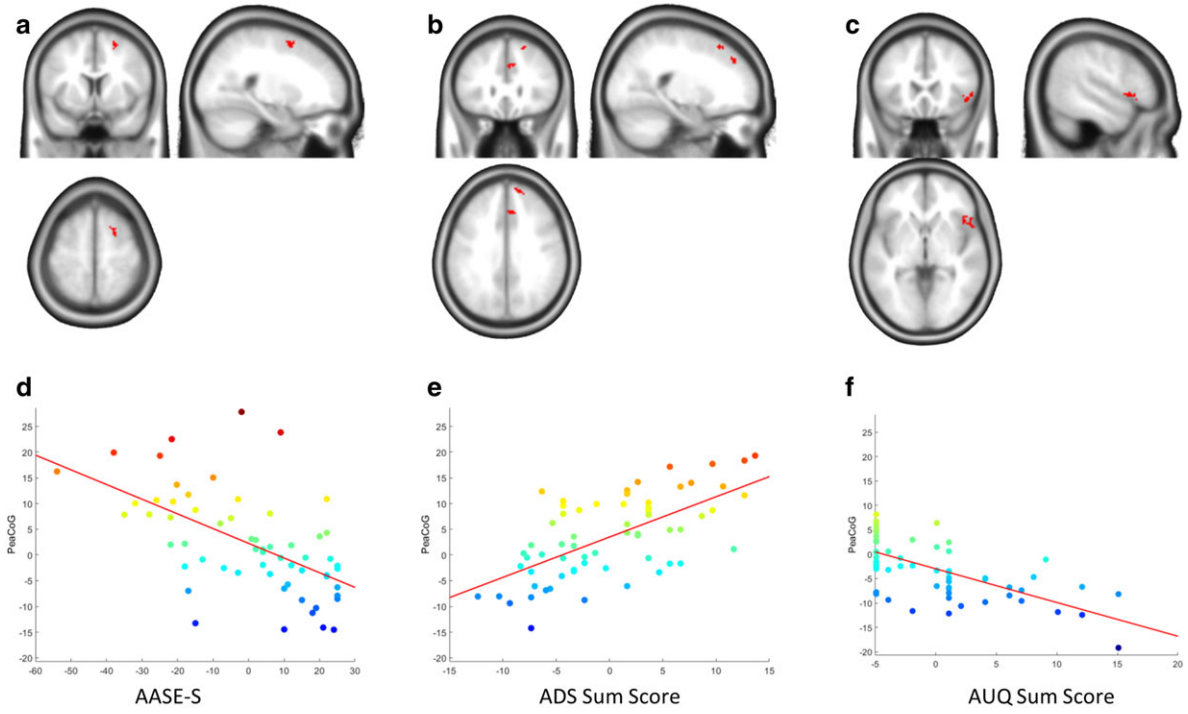

FIGURE 3 Association with clinical variables. Clusters where striatal peak connectivity location on the gradient (PeaCoG) was associated with clinical self-report questionnaires (cluster-level $P < 0.025$ corr.) in the AUD sample. Association with (a) the AASE self-efficacy to abstain (AASE-S) scale, (b) the alcohol dependence scale (ADS) sum score, and (c) the alcohol urge questionnaire (AUQ) sum score. DEF scatter plots of the respective effects. AASE-S: Alcohol abstinence self-efficacy scale self-efficacy to abstain, ADS: Alcohol dependence scale, AUQ: Alcohol urge questionnaire. The color scale corresponds to the striatal gradient in Figure 1A

were not significantly associated ($P < 0.05$ uncorr.) with any clinical variable in the AUD group after exclusion of one outlier (>5 SD above the group mean).

4 | DISCUSSION

In this study, we characterized each voxel in the frontal cortex by the location of strongest resting state functional connectivity with the striatum along an empirically estimated frontostriatal connectivity gradient, compared these effects between participants with alcohol use disorder and healthy controls, and assessed associations with clinical variables.

First of all, it is noteworthy that the striatal medial-ventral-rostral to lateral-dorsal-caudal gradient (Figure 1A) we estimated empirically from fMRI data is consistent with previous literature based on nonhuman primate tract tracing studies.[1] The mean connectivity profile in

the ventral part of the frontal cortex is exhibiting the pattern described in the literature (Figure 1B), supporting the assumption that this gradient represents a general organizational principle of frontostriatal projections.

The dorsal part of the frontal cortex has more medial mean connectivity which seems to violate the expected pattern (Figure 1B) but might be related to the higher standard deviation in dorsal parts of the frontal cortex (Figure S3). Furthermore, more dorsal areas potentially have motor-related functions that are probably less active when participants lie still in the scanner, which might dampen the operative component of these motor circuits. Overall, we identified a substantial amount of interindividual variability of peak connectivity locations along the gradient (Figure S3), showing that frontal regions indeed differ with respect to the striatal regions they are most strongly interacting with.

On the basis of PeaCoG values, we identified a cluster in the rOFC with more ventral striatal peak connectivity in AUD, suggesting a stronger integration with more ventral striatal regions (Figure 2A). Importantly, while we identified this cluster due to a mean difference, the underlying effect might rather be characterized as reduced variability in the integration of the rOFC with the striatum (Figure 2B). This effect could be interpreted as a "clamping" of the rOFC to the ventral striatum or termed in the framework of Shipp,[3] a bias towards the "operative"component of rOFC-striatal connectivity in comparison to "contextual" influences in healthy controls. This interpretation is in line with models proposing that compulsive consumption of substances is related to dysfunctions of the OFC-striatal circuit.[40] Volkow and Fowler[40] argue that activation of the OFC leads to an intense urge or drive to consume, despite conflicting signals not to. Dopamine release during intoxication strengthens this circuit and leads to a loss of control and thus preservation of compulsive alcohol intake.

We did not find an association of the rOFC cluster with clinical self-report questionnaires. We can only speculate that because of the small variance within the AUD group, it might have been infeasible to identify a significant association with disorder-specific self-report measures. However, we identified associations of striatal peak connectivity locations with clinical variables in the right superior frontal gyrus, medial frontal cortex, DLPFC, and inferior frontal cortex. Here, the different questionnaires identified distinct and nonoverlapping clusters likely reflecting the diverse aspects of AUD symptomology the questionnaires are measuring.

In the superior frontal gyrus, more ventral PeaCoG values were associated with self-efficacy to abstain from future drinking. Here, it might be the case that more dorsal connectivity of the superior frontal gyrus is associated with the experience of less control over drinking behavior and less optimism because it might reflect the "operative" component of dorsal striatal circuits, which are related to more habitual, automatic responses to alcohol stimuli.[15]

PeaCoG values in the medial frontal and dorsolateral prefrontal regions were associated with alcohol dependence (ADS scale), which likely reflects frontal control processes[10,13] where more ventral peak connectivity represent stronger prefrontal control over reward-related circuits of the striatum. For example, Park et al[41] have found that impaired functional connectivity between the VS and the DLPFC in a reward-guided decision-making task was associated with learning impairments and alcohol craving. In monetary reward task data of our subjects, we also found that task-dependent connectivity changes between the VS and an adjacent DLPFC cluster were impaired[34] and that VS reward sensitivity was predictive for therapy-related activation changes in another adjacent DLPFC cluster.[33]

More ventral rIFG peak connectivity was associated with the urge to drink alcohol. Disruption of the IFG has been associated with dysfunctional response inhibition and impulse control, where the IFG fails to act as a brake over response tendencies.[42] This brake could be turned on in different modes (response suppression) and in different contexts (external signals, goals).[43] In our participants, an increased urge to consume alcohol might thus require increased inhibitory control of the rIFG over reward-related ventral striatal regions.

Notably, several limitations apply to our study. First of all, our clinical sample comprises participants with AUD in a specific period of 5 to 31 days abstinence, and our results might be specific for this period. Furthermore, with our analyses, we are not able to differentiate whether the detected effects are representing a risk factor or a consequence of the disorder.

Because our analyses depend on the exact location of voxels, we decided to include the individual size of the target structures in native space as covariates. This is especially relevant in a clinical sample like ours where anatomical damage can be expected at least in some participants. The covariates did not change the results, suggesting that individual differences in the size of the brain structures do not play a confounding role in our analyses.

We used the peak voxel as the exactly defined point in the striatum frontal regions are most strongly interacting with. However, this is a massive data reduction step that reduces the available information and possesses the risk of increasing the noise and reduces the stability of the readout. To test for the stability of peak voxel selection, we rerun the analyses with an additional cluster constraint and selected the peak voxel only from clusters of $k = 5$ voxels with maximal connectivity, which excludes peak voxels not neighboring other voxels with maximal connectivity. These control analyses identified the same clusters (results not reported), demonstrating that our results are not overly influenced by noise from the peak voxel selection procedure.

Also, choosing a single linear gradient per hemisphere to characterize frontostriatal connectivity is certainly a simplification of the real underlying structure and might dismiss potentially interesting information. However, even by choosing the simplest linear approach, we can explain approximately 64% variance of the mean connectivity pattern. Furthermore, with our approach, we are able to detect meaningful results in dorsal, medial, and ventral parts of the frontal cortex that are straightforward to interpret and fit well with previous addiction-related research.

An open question is the correspondence of our functional connectivity measure to anatomical white matter tracts. While we expect peak connectivity locations to be constrained by the underlying anatomical connectivity, we do not have the respective tractography data to test this in the data set at hand. This will be an important test to verify the validity of the approach in the future.

After exclusion of female participants, we were not able to reach our statistical detection threshold in the group comparison. Thus, we cannot exclude that the detected mean group difference was

influenced by an excess of female participants in the control group. However, the failed detection might, at least to a certain degree, be attributable to a loss of power as the effect size diminished only slightly, and the effect was still present in a post-hoc ROI analysis restricted to the cluster. Furthermore, the observation that the rOFC had reduced variability in the AUD group was robust and still highly significant within the male participants only (Supplementary Figure S4).

The OFC is notorious for data loss in fMRI studies. While we excluded subjects with restricted coverage of the whole brain in normalized data, a reduced signal in the OFC in the clinical group might have an influence on the group comparison. Therefore, we calculated the amplitude of the fast Fourier transformed signal in the rOFC cluster in the frequency range of 0.01 to 0.1 Hz, which is considered the most relevant for resting state BOLD oscillations. This value is also called Amplitude of Low Frequency Fluctuations (ALFF[44]). The amplitude of the rOFC signal was considerably larger in the clinical group than in the control group (two sample t test, $t = 2.35$, $P = 0.01$) and associated with more ventral striatal peak connectivity over all subjects after correction for the group effect (GLM, $t = 3.67$, $P < 0.001$). This suggests that patients have stronger signal fluctuations in the rOFC cluster, which are related to more ventral striatal peak connectivity but not a reduced signal.

It might also be possible that the results of the group comparison are confounded by higher variability in the patient data. However, higher variability or data loss in the patients could be expected to increase the variability of the results. This would be opposite to the higher variability in striatal peak connectivity in the healthy control group that we found (Figure 2B).

Here, we selectively focused on frontostriatal connectivity in AUD because the striatum is a homogenous region with a topographical connectivity pattern. This provides only a partial view on the complex cortical and subcortical adaptations related to addiction.[45] An important subcortical region for addiction is for example the amygdala. Decreases in amygdala-frontal cortex resting state connectivity are related to and predictive for alcohol use.[46,47]

It further remains open how specific our results are for AUD. It will be interesting to test whether similar or divergent effects exist in other mental disorders and especially in disorders with compulsive behavior. For example, resting state alterations in frontostriatal connectivity have also been described in internet addiction disorder.[48]

Overall, our results provide insight into the functional adaptations of frontostriatal circuits that are involved in alcohol addiction, have the potential to inform future hypotheses about frontostriatal connectivity, and might provide promising targets for novel treatment approaches for alcohol use disorder by real-time fMRI neurofeedback.[49,50]

ACKNOWLEDGEMENTS

The study was funded by the Deutsche Forschungsgemeinschaft (SFB 636/D6). In addition, portions of this work were supported by grants from the German Bundesministerium für Bildung und Forschung to FK (BMBF, 01ZX1311A) and PK (BMBF, 01GQ1003B) and funding from the European Union's Horizon 2020 Framework Programme under grant agreement No 668863 (SyBil-AA).

CONFLICT OF INTEREST

The authors declare no conflict of interest.

AUTHORS CONTRIBUTION

P.K., F.K., and M.K. were responsible for the study concept and design. A.B. and M.K. collected the data. M.F.G. developed the analysis approach and analyzed the data. M.F.G., A.B., and P.K. assisted with interpretation of findings and drafted the manuscript. F.K. and M.K. provided critical revision of the manuscript for important intellectual content. All authors critically reviewed content and approved the final version for publication.

ORCID

Martin Fungisai Gerchen http://orcid.org/0000-0003-3071-5296
Falk Kiefer http://orcid.org/0000-0001-7213-0398
Peter Kirsch http://orcid.org/0000-0002-0817-1248

REFERENCES

1. Haber SN. The primate basal ganglia: parallel and integrative networks. *J Chem Neuroanat*. 2003;26(4):317-330.
2. Haber SN. Corticostriatal circuitry. *Dialogues Clin Neurosci*. 2016;18(1):7-21.
3. Shipp S. The functional logic of corticostriatal connections. *Brain Struct Funct*. 2017;222(2):669-706.
4. Forbes EE, Rodriguez EE, Musselman S, Narendran R. Prefrontal response and Frontostriatal functional connectivity to monetary reward in abstinent alcohol-dependent young adults. *PLoS One*. 2014;9(5):e94640.
5. Goldstein RZ, Volkow ND. Dysfunction of the prefrontal cortex in addiction: neuroimaging findings and clinical implications. *Nat Rev Neurosci*. 2011;12(11):652-669.
6. Akine Y, Kato M, Muramatsu T, et al. Altered brain activation by a false recognition task in young abstinent patients with alcohol dependence. *Alcohol Clin Exp Res*. 2007;31(9):1589-1597.
7. Goldstein RZ, Leskovjan AC, Hoff AL, et al. Severity of neuropsychological impairment in cocaine and alcohol addiction: association with metabolism in the prefrontal cortex. *Neuropsychologia*. 2004;42(11):1447-1458.
8. Goldstein RZ, Volkow ND. Drug addiction and its underlying neurobiological basis: neuroimaging evidence for the involvement of the frontal cortex. *Am J Psychiatry*. 2002;159(10):1642-1652.
9. Li CR, Luo X, Yan P, Bergquist K, Sinha R. Altered impulse control in alcohol dependence: neural measures of stop signal performance. *Alcohol Clin Exp Res*. 2009;33(4):740-750.
10. Camchong J, Stenger VA, Fein G. Resting state synchrony in short-term versus long-term abstinent alcoholics. *Alcohol Clin Exp Res*. 2013b;37(5):794-803.
11. Müller-Oehring EM, Jung Y-C, Pfefferbaum A, Sullivan EV, Schulte T. The resting brain of alcoholics. *Cereb Cortex*. 2015;25(11):4155-4168.
12. Zhu X, Cortes CR, Mathur K, Tomasi D, Momenan R. Model-free functional connectivity and impulsivity correlates of alcohol dependence: a resting-state study. *Addict Biol*. 2017;22(1):206-217.
13. Camchong J, Stenger A, Fein G. Resting-state synchrony during early alcohol abstinence can predict subsequent relapse. *Cereb Cortex*. 2013a;23(9):2086-2099.
14. Everitt BJ, Robbins TW. Drug addiction: updating actions to habits to compulsions ten years on. *Annu Rev Psychol*. 2016;67(1):23-50.
15. Vollstädt-Klein S, Wichert S, Rabinstein J, et al. Initial, habitual and compulsive alcohol use is characterized by a shift of cue processing from ventral to dorsal striatum. *Addiction*. 2010;105(10):1741-1749.

16. Choi EY, Yeo BTT, Buckner RL. The organization of the human striatum estimated by intrinsic functional connectivity. *J Neurophysiol*. 2012;108(8):2242-2263.
17. Di Martino A, Scheres A, Margulies DS, et al. Functional connectivity of human striatum: a resting state fMRI study. *Cereb Cortex*. 2008;18(12):2735-2747.
18. Draganski B, Kherif F, Klöppel S, et al. Evidence for segregated and integrative connectivity patterns in the human basal ganglia. *J Neurosci*. 2008;28(28):7143-7152.
19. Jeon H-A, Anwander A, Friederici AD. Functional network mirrored in the prefrontal cortex, caudate nucleus, and thalamus: high-resolution functional imaging and structural connectivity. *J Neurosci*. 2014;34(28):9202-9212.
20. Robinson JL, Laird AR, Glahn DC, et al. The functional connectivity of the human caudate: an application of meta-analytic connectivity modeling with behavioral filtering. *Neuroimage*. 2012;60(1):117-129.
21. Verstynen TD, Badre D, Jarbo K, Schneider W. Microstructural organizational patterns in the human corticostriatal system. *J Neurophysiol*. 2012;107(11):2984-2995.
22. Averbeck BB, Lehman J, Jacobson M, Haber SN. Estimates of projection overlap and zones of convergence within frontal-striatal circuits. *J Neurosci*. 2014;34(29):9497-9505.
23. Barnes KA, Cohen AL, Power JD, et al. Identifying basal ganglia divisions in individuals using resting-state functional connectivity MRI. *Front Syst Neurosci*. 2010;4:18.
24. Jarbo K, Verstynen TD. Converging structural and functional connectivity of orbitofrontal, dorsolateral prefrontal, and posterior parietal cortex in the human striatum. *J Neurosci*. 2015;35(9):3865-3878.
25. Jung WH, Jang JH, Park JW, et al. Unravelling the intrinsic functional organization of the human striatum: a parcellation and connectivity study based on resting-state fMRI. *PLoS One*. 2014;9(9):e106768.
26. Selemon L, Goldman-Rakic P. Longitudinal topography and interdigitation of corticostriatal projections in the rhesus monkey. *J Neurosci*. 1985;5(3):776-794.
27. Yeterian EH, Van Hoesen GW. Cortico-striate projections in the rhesus monkey: the organization of certain cortico-caudate connections. *Brain Res*. 1978;139(1):43-63.
28. First MB, Spitzer RL, Gibbon M, Williams JB. Structured Clinical Interview for DSM-IV Axis I Disorders: *Patient* Edition (February 1996 Final), SCID-I/P. Biometrics Research Department, New York State Psychiatric Institute; 1998.
29. Anton RF. Obsessive–compulsive aspects of craving: development of the obsessive compulsive drinking scale. *Addiction*. 2000;95:211-217.
30. DiClemente CC, Carbonari JP, Montgomery RP, Hughes SO. The alcohol abstinence self-efficacy scale. *J Stud Alcohol*. 1994;55(2):141-148.
31. Skinner HA, Horn JL, Ontario ARF. *Alcohol Dependence Scale (ADS) User's Guide*. Addiction Research Foundation; 1984.
32. Bohn MJ, Krahn DD, Staehler BA. Development and initial validation of a measure of drinking urges in abstinent alcoholics. *Alcohol Clin Exp Res*. 1995;19(3):600-606.
33. Becker A, Gerchen MF, Kirsch M, Hoffmann S, Kiefer F, Kirsch P. Striatal reward sensitivity predicts therapy-related neural changes in alcohol addiction. *Eur Arch Psychiatry Clin Neurosci*. 2018;268(3):231-242.
34. Becker A, Kirsch M, Gerchen MF, Kiefer F, Kirsch P. Striatal activation and frontostriatal connectivity during non-drug reward anticipation in alcohol dependence. *Addict Biol*. 2017;22(3):833-843.
35. Buuren M, Gladwin TE, Zandbelt BB, et al. Cardiorespiratory effects on default-mode network activity as measured with fMRI. *Hum Brain Mapp*. 2009;30:3031-3042.
36. Winkler AM, Ridgway GR, Webster MA, Smith SM, Nichols TE. Permutation inference for the general linear model. *Neuroimage*. 2014;92:381-397.
37. Smith SM, Nichols TE. Threshold-free cluster enhancement: addressing problems of smoothing, threshold dependence and localisation in cluster inference. *Neuroimage*. 2009;44(1):83-98.
38. Brown MB, Forsythe AB. Robust tests for the equality of variances. *J Am Stat Assoc*. 1974;69(346):364-367.
39. Olejnik SF, Algina J. Type I error rates and power estimates of selected parametric and nonparametric tests of scale. *J Educ Stat*. 1987;12(1):45-61.
40. Volkow ND, Fowler JS. Addiction, a disease of compulsion and drive: involvement of the orbitofrontal cortex. *Cereb Cortex*. 2000;10(3):318-325.
41. Park SQ, Kahnt T, Beck A, et al. Prefrontal cortex fails to learn from reward prediction errors in alcohol dependence. *J Neurosci Off J Soc Neurosci*. 2010;30(22):7749-7753.
42. Hampshire A, Chamberlain SR, Monti MM, Duncan J, Owen AM. The role of the right inferior frontal gyrus: inhibition and attentional control. *Neuroimage*. 2010;50(3):1313-1319.
43. Aron AR, Robbins TW, Poldrack RA. Inhibition and the right inferior frontal cortex: one decade on. *Trends Cogn Sci*. 2014;18(4):177-185.
44. Zang YF, He Y, Zhu CZ, et al. Altered baseline brain activity in children with ADHD revealed by resting-state functional MRI. *Brain Dev*. 2007;29(2):83-91.
45. Volkow ND, Koob GF, McLellan AT. Neurobiologic advances from the brain disease model of addiction. *N Engl J Med*. 2016;374(4):363-371.
46. Peters S, Jolles DJ, Van Duijvenvoorde AC, Crone EA, Peper JS. The link between testosterone and amygdala-orbitofrontal cortex connectivity in adolescent alcohol use. *Psychoneuroendocrinology*. 2015;53:117-126.
47. Peters S, Peper JS, Van Duijvenvoorde ACK, Braams BR, Crone EA. Amygdala-orbitofrontal connectivity predicts alcohol use two years later: a longitudinal neuroimaging study on alcohol use in adolescence. *Dev Sci*. 2017;20(4).
48. Lin F, Zhou Y, Du Y, et al. Aberrant corticostriatal functional circuits in adolescents with internet addiction disorder. *Front Hum Neurosci*. 2015;9.
49. Gerchen MF, Kirsch M, Bahs N, et al. The SyBil-AA real-time fMRI neurofeedback study: protocol of a single-blind randomized controlled trial in alcohol use disorder. *BMC Psychiatry*. 2018;18(1):12.
50. Kirsch M, Gruber I, Ruf M, Kiefer F, Kirsch P. Real-time functional magnetic resonance imaging neurofeedback can reduce striatal cue-reactivity to alcohol stimuli. *Addict Biol*. 2016;21(4):982-992.

SUPPORTING INFORMATION

Additional supporting information may be found online in the Supporting Information section at the end of the article.

How to cite this article: Gerchen MF, Rentsch A, Kirsch M, Kiefer F, Kirsch P. Shifts in the functional topography of frontal cortex-striatum connectivity in alcohol use disorder. *Addiction Biology*. 2019;24:1245–1253. https://doi.org/10.1111/adb.12692